

Evolution of CO₂ during Birnessite-Induced Oxidation of ¹⁴C-Labeled Catechol

Emily H. Majcher, Jon Chorover,* Jean-Marc Bollag, and P. M. Huang

ABSTRACT

Phenolic compounds undergo several transformation processes in soil and water (i.e., partial degradation, mineralization, and polymerization), many of which have been attributed primarily to biological activity. Results from previous work indicate that naturally occurring Mn oxides are also capable of oxidizing phenolic compounds. In the present study, ¹⁴C-labeled catechol was reacted with birnessite (manganese oxide) in aqueous suspension at pH 4. The mass of catechol-derived C in solid, solution, and gas phases was quantified as a function of time. Between 5 and 16% of the total catechol C was liberated as CO₂ from oxidation and abiotic ring cleavage under various conditions. Most of the ¹⁴C (55–83%) was incorporated into the solid phase in the form of stable organic reaction products whereas solution phase ¹⁴C concentrations increased from 16 to 39% with a doubling of total catechol added. Polymerization and CO₂ evolution appear to be competitive pathways in the transformation of catechol since their relative importance was strongly dependent on initial birnessite–catechol reaction conditions. Solid phase Fourier transform infrared (FTIR) spectra are consistent with the presence of phenolic, quinone, and aromatic ring cleavage products. Carbon dioxide release appears to be limited by availability of reactive birnessite surface sites and it is diminished in the presence of polymerized reaction products.

IT HAS LONG BEEN RECOGNIZED that intracellular and extracellular enzymes of microorganisms and plants are directly involved in the degradation of organic compounds in soils. These enzymes (e.g., oxidoreductase, hydrolase, and dehalogenase) mediate transformations of both naturally occurring and anthropogenic organic compounds, producing various intermediate products of the humification process (Bollag et al., 1988, 1995). Many naturally occurring and anthropogenic organic compounds (e.g., polycyclic aromatic hydrocarbons, phenols, benzenes, and cresols) undergo enzymatic dioxygenation before any aromatic ring fission and CO₂ evolution occurs (Dagley, 1971; Reineke and Knackmuss, 1988). As a result, catechol (1,2-dihydroxybenzene) is found in soils as an organic matter constituent, plant polyphenol, and an intermediate of microbial metabolism of xenobiotics (Martin et al., 1979).

Previous research has established that abiotic soil constituents, including manganese and iron (hydr)oxides, react with organic compounds, analogous to enzyme-mediated transformation, yielding humic substances (Shindo and Huang, 1982, 1984; McBride, 1987, 1989a,b; Huang, 1991). Oxidation of aromatic compounds by Mn (hydr)oxide surfaces is thought to result sequentially from (i) bonding of the organic to the surface through phenolic-OH or carboxylic functional groups, (ii) elec-

tron transfer from the organic to oxide, and (iii) release of the reduced metal (Stone and Morgan, 1984b). For dihydroxybenzenes (e.g., catechol), semiquinone radicals and quinones are formed prior to further oxidation and/or polymerization. Prevalence of semiquinone radicals increases with increasing pH and their oxidation to quinones is correlated with O₂ consumption (McBride, 1989a,b). McBride (1989a) did not observe radical products in birnessite–catechol suspensions buffered at pH 5.4 and O₂ consumption over the course of the experiment was insignificant, indicating that Mn(IV) is the primary oxidant in acidic systems.

Recently, it has been shown that there is a complementary or competing mechanism resulting in aromatic ring cleavage and liberation of CO₂ from these non-biological systems (Wang and Huang, 1994; Wang, 1995; Lee and Huang, 1995; Cheney et al., 1996, 1998). Although mineral dissolution and phenolic polymerization have been well documented, the kinetics and mechanisms of the simultaneous release of CO₂ remain to be established. In particular, the rate and relative magnitude of ¹⁴CO₂ release from radiolabeled parent compounds have not been evaluated previously. Therefore, the objectives of this study were (i) to quantify the mass of catechol-derived C in solid, solution, and gas phases as a function of time and (ii) to confirm that CO₂ release from the catechol–birnessite system is derived from ring cleavage of catechol. We measured ¹⁴CO₂ evolution at acidic pH such that Mn(IV) was the primary oxidant. The effect of adding fresh birnessite and/or catechol after a specified reaction time was used to elucidate processes limiting CO₂ release.

MATERIALS AND METHODS

Birnessite (manganese oxide) was synthesized by adding concentrated hydrochloric acid to a boiling solution of potassium permanganate (McKenzie, 1971). The precipitate was washed repeatedly with distilled deionized water until the wash solution tested negative for Cl⁻. Analysis of the freeze-dried precipitate by x-ray diffraction indicated a poorly crystalline mineral with *d*-spacings of 0.7121, 0.3582, and 0.2432 nm (in decreasing intensity) characteristic of synthetic birnessite (McKenzie, 1989). Manganese content of the oxide was found to be 580 g kg⁻¹ following dissolution in acidified hydroxylamine hydrochloride (Chao, 1972). The birnessite was sterilized by ⁶⁰Co γ-irradiation prior to experiments (Nuclear Reactor Facility, University Park, PA).

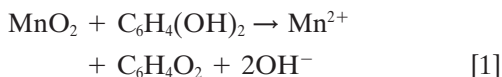
Reagent grade catechol and uniformly ¹⁴C-labeled catechol (98% purity, specific activity of 17.7 mCi mmol⁻¹) were purchased from Sigma (St. Louis, MO) and used in experiments with birnessite. All inorganic chemicals used were reagent grade and all solutions were prepared with filter-sterilized, distilled, deionized water.

Preliminary experiments in low ionic strength NaCl solu-

E.H. Majcher, J. Chorover, and J.-M. Bollag, Dep. of Agronomy and Center for Bioremediation and Detoxification, The Pennsylvania State Univ., University Park, PA 16802; P.M. Huang, Dep. of Soil Science, Univ. of Saskatchewan, Saskatoon, SK S7N 5A8. Received 12 March 1999. *Corresponding author (jdc7@psu.edu).

Abbreviations: FTIR, Fourier transform infrared; DRIFT, diffuse reflectance infrared Fourier transform.

tions indicated large pH increases resulting from the reaction of catechol and birnessite because of the production of hydroxide ions with 1,2-benzoquinone as shown in Eq. [1]



In the absence of buffer solutions, the increase in pH is accompanied by significant O₂ consumption (McBride, 1987). Oxygen consumption may result from autocatalytic oxidation of Mn²⁺ (favored at alkaline pH) and oxidation of semiquinone radical intermediates by O₂. In the latter case, the relative contribution of Mn⁴⁺ and O₂ to catechol oxidation is not clear. We found that O₂ consumption was negligible—decreasing by less than 5% over the first hour of reaction—when birnessite and catechol were reacted at pH 4 in buffered, closed systems that were initially saturated with lab air (21% O₂). Similarly, McBride (1989b) showed that at pH 5.4, surface Mn(IV) is the primary electron acceptor even in oxic conditions. All of our experiments were conducted at pH 4, in 0.1 M Na-acetate buffer solution, to assure that Mn(IV) was the primary electron acceptor. Acetate buffer was selected because it is less reactive with the birnessite surface than alternatives (e.g., phosphate-citrate, Universal) (Stone, 1987). In experimental controls, we confirmed that the buffer alone did not induce measurable dissolution of birnessite.

Experimental Conditions

All experiments were conducted in triplicate for 24 h in aerated, continuously mixed batch reactors. Each reactor consisted of a sealed 250-mL Erlenmeyer flask supplied with air that was stripped of ambient CO₂ by bubbling through a series of three test tubes containing 3 mol L⁻¹ NaOH solution. Effluent ¹⁴CO₂ evolving from the reaction was trapped in a series of three 0.1 mol L⁻¹ NaOH traps placed downstream of the reaction vessel. Nearly all of the ¹⁴CO₂ was trapped in the first two of the effluent NaOH traps. Continuous aeration was maintained by drawing a vacuum on the effluent end of the air stream. The initial catechol and birnessite concentrations were 2.3 mmol L⁻¹ (13.8 mmol L⁻¹ as C) and 1.0 g L⁻¹, respectively, to give a Mn(IV) to catechol molar ratio of 4.54. Total volume of the suspension was 125 mL. The distribution of ¹⁴C among solid, aqueous and gaseous phases was measured as a function of time over 24 h.

To elucidate factors controlling CO₂ evolution, three additional treatments were examined. Batch systems were constructed exactly as above for the starting conditions but, after a 5-h reaction time, a second pulse addition (of concentration equal to the first) of birnessite, catechol, or both birnessite and catechol was added. Hereafter, these experiments are referred to as “+B”, “+C” and “+BC”, respectively. The baseline case (no pulse addition at 5 h) is referred to as “+0”.

Unlabeled catechol stock was mixed with uniformly labeled ¹⁴C catechol (to give a total catechol concentration of 2.3 mmol L⁻¹ and a ¹⁴C concentration of 2.0 × 10⁴ DPM mL⁻¹) prior to addition to pre-mixed aqueous birnessite suspensions. The concentration of ¹⁴C in solution, solid and gas (¹⁴CO₂) phases was measured at six different times over a 24-h reaction period (1, 2, 5, 6, 9, 24 h). At each sampling time, a 10-mL aliquot was removed from the flask through a syringe and centrifuged for 20 min at 12 500 g with a Sorvall Superspeed RC2-B centrifuge (Sorvall Instruments - Du Pont Company, Newton, CT). The supernatant solution and pellet were separated for further analysis.

Chemical Analysis

A 0.100-mL sample of the supernatant solution was mixed with 10 mL of Eco-Scint scintillation cocktail (National Diag-

nostics, Atlanta, GA) and radioactivity was determined by a Beta Trac 6895 liquid scintillation counter (Elk Grove, IL). The pellet was air dried in a vacuum desiccator for at least 24 h prior to combustion in a Harvey Biological Oxidizer OX 600 (Hillsdale, NJ) using Harvey Carbon 14 Cocktail (Hillsdale, NJ) for absorption of ¹⁴CO₂. Radioactivity of the solid phase was then determined in a Beta Trac 6895 liquid scintillation counter and corrected for contributions due to entrained solution.

Evolution of ¹⁴CO₂ was monitored by collection in three successive 0.5 M NaOH traps (each 5 mL in volume) in the flow of air leaving the batch reactor and connected by glass tubing. Sodium hydroxide solutions were collected quantitatively at each sampling time and replaced with fresh NaOH. Trap solutions were combined, vigorously mixed, and a 0.5-mL sub-sample was combined with Eco-Scint cocktail for determination of ¹⁴CO₂. Experiments were conducted in duplicate or triplicate and control reactors (no birnessite added) were used to determine initial radioactivity (time = 0 h) and any loss of ¹⁴C over time.

Aliquots of the supernatant solution were analyzed by HPLC to measure catechol concentration. A 1.0 mL sample of the supernatant solution was filtered through a 0.45 μm membrane filter (Millipore Corp., Milford, MA), followed by 4 mL of water and 5 mL of methanol to a final eluate volume of 10 mL. The filtrate was thoroughly mixed and triplicate aliquots were injected into a Waters Associates HPLC system (Waters Corp., Milford, MA) equipped with two model 510 pumps, model 717 autosampler, and a Lambda Max 440 absorbance detector set at 254 nm. A solvent system of 60% methanol and 40% distilled deionized water was passed isocratically at a flow rate of 0.8 mL min⁻¹ through a 30 cm, hyperchrome reverse phase C-18 Nucleosil column for analyte separation (Supelco, Bellefonte, PA).

Solution samples were analyzed by flame atomic absorption spectrometry (AAS, Thermo Optek Corp., Atlanta, GA) to determine time-dependent changes in Mn concentration. Aliquots were first filtered through a 0.2-μm membrane filter disk (Gelman Science, Fisher Scientific, Pittsburgh, PA) to remove colloidal Mn. Control experiments, conducted in the absence of catechol, confirmed negligible dissolution of Mn in pH 4 acetate buffer over 24 h.

Diffuse Reflectance Infrared Fourier Transform (DRIFT) Spectroscopy

Each pellet was washed twice with 0.01 M NaCl solution to remove entrained solution and then freeze-dried in a Lab-conco (Lyph-Lock 6) Freeze Dry System (Fisher Scientific, Pittsburgh, PA) prior to analysis by DRIFT spectroscopy on a Nicolet Magna 560 FTIR spectrometer (Nicolet Instrument Corp., Madison, WI). DRIFT samples were prepared by grinding 14 mg of sample with 60 mg KBr for 40 s. An additional 360 mg of KBr were ground with the sample with a Wig-L-Bug (Spex Sample Preparation, Metuchen, NJ), bringing the final concentration of the freeze-dried sample to 3% (w/w). Solid samples from each of the four treatment conditions (+0, +C, +B, +BC) after the 24-h reaction time were analyzed with a minimum of 400 scans and 4 cm⁻¹ resolution. Spectra of birnessite before and after reaction with acetate buffer for 24 h were identical, indicating that interaction with the acetate buffer in the absence of catechol had no FTIR detectable effect on the Mn oxide. Difference spectra of the organic reaction products were obtained following subtraction of the birnessite spectrum.

Selected experiments were conducted under sterile conditions to verify the abiotic nature of the reactions. Glassware

and solutions were autoclaved and all aliquots were removed from suspension in a sterile UV hood. Suspension samples were plated on nutrient agar and incubated for 48 h at 35°C to confirm the absence of microbial growth.

RESULTS

The use of ¹⁴C labeled catechol aids in tracking the mass of catechol-derived carbon through solid, solution, and gas phases over the 24-h reaction time. Figure 1 displays the phase distribution of carbon in the baseline reaction of catechol and birnessite. In these experiments, no subsequent additions were made to the batch reactors. Since 1 mole of catechol corresponds to 6 moles of carbon, the reaction began with 13.8 mmol L⁻¹ as C. Control assays (no birnessite) resulted in minimal (<3%) loss of catechol from solution (Majcher, 1998). Results of the experiment conducted under normal (Fig. 1a) and strict sterile (Fig. 1b) conditions differed only slightly, confirming that the reaction was indeed abiotic. Dissolved catechol concentration (measured by HPLC) was reduced from 2.3 mmol L⁻¹ (13.8 mmol L⁻¹ as C) to 0.3 mmol L⁻¹ (1.8 mmol L⁻¹ as C) within the first hour of reaction and to below HPLC detection limits (10 μmol L⁻¹) within 2 h. Comparison of these HPLC results with the ¹⁴C data on total soluble C indicates that a significant amount of ¹⁴C remaining in solution after 2 h of reaction time was not catechol, but rather a transformation product of the parent compound (Fig. 1). Nonetheless, within 2 h, catechol-derived C decreased to 2.96 ± 0.33 mmol L⁻¹ in solution and increased to 4.76 ± 0.45 mmol L⁻¹ in the solid phase, while only a small fraction (0.3 ± 0.2 mmol L⁻¹) was released as CO₂.

Solution and solid concentrations stabilized after 5 h. At the end of 24 h, these values were 2.19 ± 0.18 and 7.22 ± 0.02 mmol L⁻¹, respectively. Carbon dioxide release continued to increase over the entire reaction time, with a cumulative release equal to 1.55 ± 0.2 mmol L⁻¹ as C, approximately 11% of the catechol-derived C in the system. The recovery of ¹⁴C in solid, liquid and gas phases ranges from 60 to 85% for Fig. 1a and 76% to 88% for Fig. 1b. In both cases, recoveries were lowest for 1- and 2-h sampling times and they improved over the course of the experiment. The low recoveries may be due to ¹⁴CO₂ loss during air drying of the pelleted solid phase in a vacuum dessicator for 24 h. Drying of the solid likely increased the extent of oxidation and associated gaseous loss of ¹⁴C. For example, Cheney et al. (1996) reported the complete abiotic degradation to CO₂ of the herbicide 2,4-dichlorophenoxyacetic acid (2,4-D) after adsorption from ethyl ether onto dry synthetic birnessite. As a result of the probable loss of ¹⁴C upon drying the solids, the solid phase concentrations of carbon may be considered to represent a lower limit.

Effects of Subsequent Birnessite and Catechol Additions

Selected experiments were conducted in a manner identical to the "baseline" experiment detailed above except that fresh birnessite and/or catechol were added

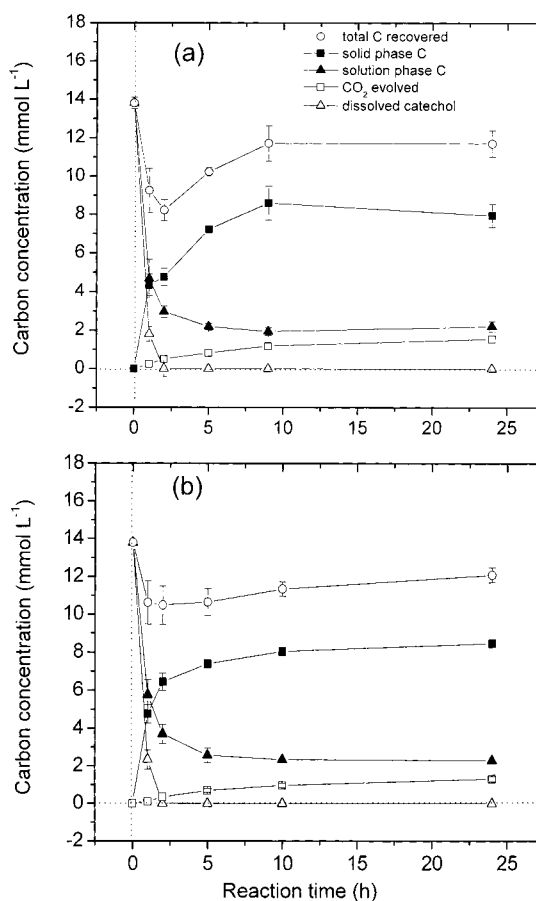


Fig. 1. Phase distribution of catechol-derived carbon as a function of time during reaction with birnessite in suspension at pH 4 (no additions at 5 h): (a) normal conditions; (b) sterile conditions. Initial catechol and birnessite concentrations were 13.8 mmol C L⁻¹ and 1.0 g L⁻¹ respectively. Mean value ± sample standard deviation is shown.

to the reaction vessels immediately after the sample aliquot was taken at 5 h. Figure 2 shows the effects of these pulse additions on the phase distribution of ¹⁴C in comparison to the baseline (+0) case. For the first 5 h of reaction, all treatments are identical and a single mean value is shown for all 12 replicates. Mean values are plotted by treatment for reaction times greater than 5 h.

The fate of newly added catechol was highly dependent upon whether or not fresh birnessite was also added. If catechol and birnessite were added together (+BC), most of the new material was rapidly incorporated into the solid phase, producing a residual solid phase concentration that was significantly higher than when catechol was added alone (Fig. 2b). When catechol alone was added at 5 h (+C), most of this material remained in solution for the duration of the experiment (Fig. 2a). Solution analyses by HPLC indicated that this soluble carbon remained in the form of unaltered catechol.

The addition of fresh birnessite alone after 5 h (+B) had no significant effect on the relatively large pool of solid phase C (Fig. 2b) and the concentration of solution phase C was not altered significantly (Fig. 2a). However,

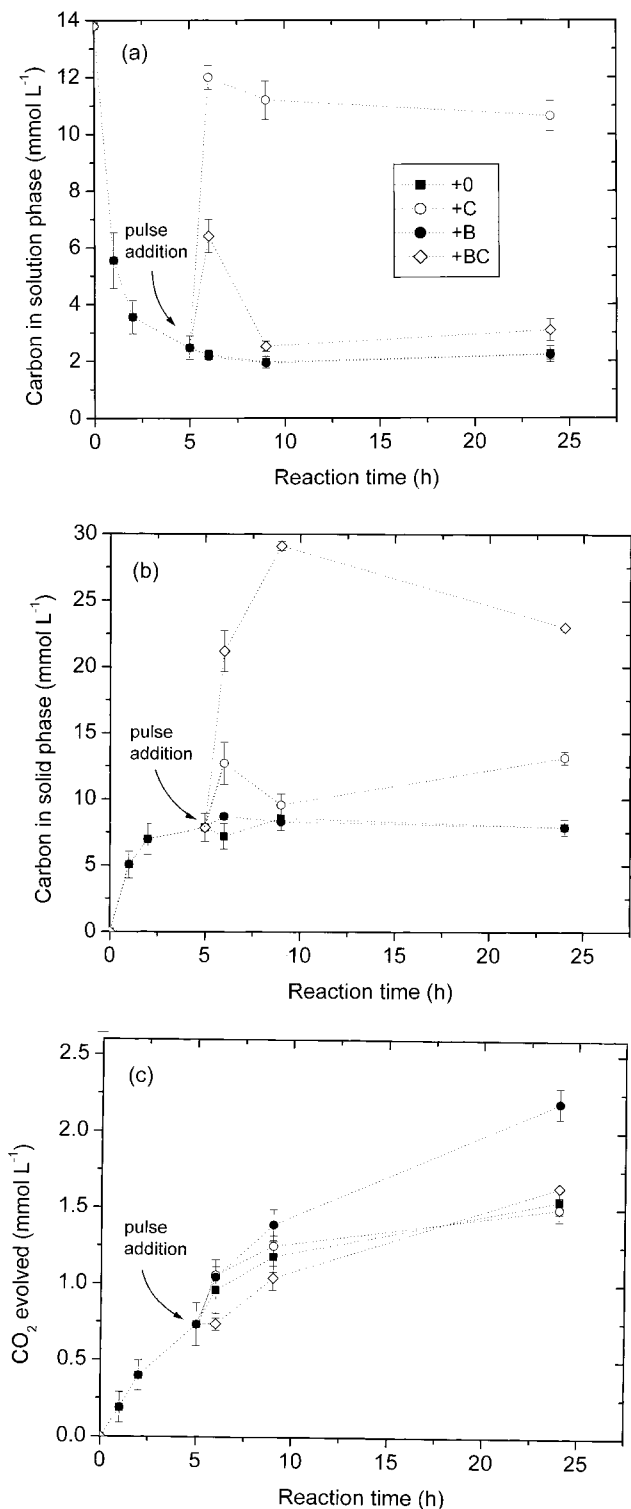


Fig. 2. Phase distribution of catechol-derived carbon as a function of time during reaction with birnessite in suspension at pH 4. Effects of second pulse of reactants [no additions (+0); catechol added (+C), birnessite added (+B) and both added (+BC)] at 5-h reaction time: (a) dissolved C; (b) solid-phase C; (c) CO₂ evolution. Initial and second pulse catechol concentrations each provided 13.8 mmol C L⁻¹. Initial and second pulse birnessite concentrations each provided 1.0 g L⁻¹. Standard deviations are indicated.

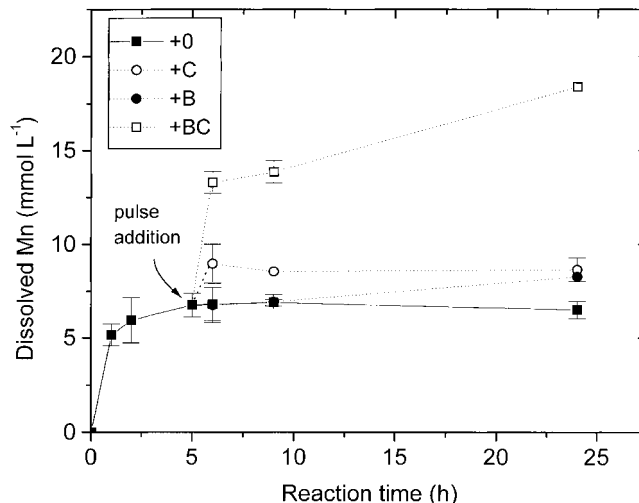


Fig. 3. Kinetics of Mn dissolution in the reaction of catechol and birnessite at pH 4. Effects of second pulse of reactants [no additions (+0), catechol added (+C), birnessite added (+B) and both added (+BC)] at 5-h reaction time. Initial and second pulse catechol concentrations each provided 13.8 mmol C L⁻¹. Initial and second pulse birnessite concentrations each provided 1.0 g L⁻¹. Standard deviations are indicated.

an increase in CO₂ evolution was observed for subsequent sampling intervals (Fig. 2c). Whereas the +0, +C and +BC treatments resulted in similar cumulative CO₂ evolution at 24 h, CO₂ release from the +B case was significantly higher. This new pulse in CO₂ evolution upon addition of birnessite alone (+B) indicates that the fresh birnessite surface (+B) was capable of oxidizing reaction products in addition to free catechol. Similarly, Naidja et al. (1998) found that CO₂ generation increased with increasing ratio of birnessite to catechol in aqueous suspension. It is important to note that additional CO₂ evolution was not observed when catechol was co-added with the birnessite at 5 h. Hence, if residual reaction products are present upon addition of fresh reactants, they appear to effectively sorb or otherwise sequester the newly oxidized materials before mineralization to CO₂ occurs.

Manganese Dissolution

Previous work has confirmed that the Mn solubilized by reaction of birnessite and catechol is predominantly in the form of Mn(II) (McBride, 1989a) and that filtration through 0.2- μ m nominal pore size filter disks effectively eliminates colloidal Mn(IV) from subsequent analyses (Stone and Morgan, 1984a,b). In our experiments, filtrate Mn in catechol-free controls was not detectable (Majcher, 1998). Therefore, time-dependent increases in soluble Mn result directly from the reduction of solid phase Mn(IV) by catechol.

Figure 3 shows the time-course solution concentration of Mn, following centrifugation and filtration, for each treatment. Prior to any secondary pulse additions to the reactors, measured Mn concentrations increased rapidly in the first hour to between 4.5 and 6 mmol L⁻¹, then stabilized through the fifth hour at approximately 7 mmol L⁻¹. Measured solution-phase concentrations

indicate that 65 to 75% of the Mn solids were dissolved over the course of 24 h. The fact that birnessite was not fully consumed during the reaction is supported by DRIFT spectra of reacted samples that showed persistence (at a lower intensity) of the broad peak at 530 to 565 cm⁻¹, which corresponds to Mn (hydr)oxide lattice vibrations.

A large increase in dissolution was detected in the +BC condition and, after 24 h, Mn concentration still appeared to be increasing. The final Mn concentration for +BC was 18.35 ± 0.21 mmol L⁻¹, which is 2.6 times greater than the +0 condition. The dissolution of Mn in +BC represents 88% of the total Mn added as birnessite. Apparently, a greater portion of the birnessite dissolved when both birnessite and catechol were co-added as a second pulse at 5 h. Since this treatment resulted in the rapid removal of ¹⁴C from solution (Fig. 2a) without a significant increase in ¹⁴CO₂ evolution over the +0 case (Fig. 2c), the large increase in Mn dissolution evidently contributes to oxidative polymerization of catechol in the residual solids (Fig. 2b).

Solid Phase Reaction Products

The oxidation of catechol by Mn(VI) solids was found to produce polymeric solid-phase residues, as has been observed previously (Huang, 1991; Naidja et al., 1998). The solubility of these materials was investigated in the present study by extracting the ¹⁴C-enriched solids (generated as a function of reaction time) sequentially in solutions of variable polarity and pH (acetate buffer solution, methanol, ethyl acetate and 0.1 M NaOH). Results are presented in Table 1. Solubility data indicate that reaction rapidly leads to the formation of highly insoluble and refractory organic precipitates. After only 2 h, less than 20% of the total ¹⁴C was solubilized by all extractants combined and most of this was extracted in the acetate buffer (Table 1). At 24 h, the 0.1 M NaOH treatment extracted the largest amount of ¹⁴C, but since this treatment removed < 10% of the total, most (90%) of the humified materials were retained in the humin fraction as insoluble birnessite complexes. The efficacy of a given solvent to extract solid-phase ¹⁴C varied with reaction time (Table 1). This suggests that the polarity of the solid-phase residue was likewise dependent on reaction time.

DRIFT spectroscopy was employed to elucidate structural composition of solid-phase organic material. The DRIFT spectrum of unreacted birnessite (not shown) contains a large peak in the 530 to 565 cm⁻¹ region from Mn-O vibrations, a broad peak at about 3500 cm⁻¹ corresponding to hydroxyl stretching, and very small peaks in the 1615 to 1630 cm⁻¹ range from adsorbed water. Functional group content of the organic reaction products was evaluated by subtracting the birnessite spectrum from that of the reacted sample. Figure 4 shows the "difference" spectra of catechol reaction products following 24-h reaction time for each treatment. All treatments exhibit a broad absorbance band around 3300 cm⁻¹ corresponding to H-bonded phenolic OH (Silverstein et al., 1991). The peaks at 1614 (+C)

Table 1. Percentage of solid-phase ¹⁴C extracted with different solvents as a function of reaction time.

Reaction time (h)	Acetate*	MeOH†	EtAc‡	NaOH#	Radioactivity in %				
2	11 ± 3.0	1.6 ± 0.17	0.7 ± 0.18	6.5 ± 0.67					
4	not avail.	3 ± 2.1	0.3 ± 0.14	7 ± 1.2					
6	1.7 ± 0.5	1.2 ± 0.6	0.7 ± 0.3	7.5 ± 0.44					
10	1.6 ± 0.7	0.9 ± 0.3	1 ± 0.5	7 ± 1.3					
24	1.8 ± 0.3	0.53 ± 0.06	0.8 ± 0.14	5.3 ± 0.2					

* Extraction with 2 mL acetate buffer solution for 5 min (pH 4).

† Extraction with 2 mL methanol for 5 min.

‡ Extraction with 2 mL ethyl acetate for 5 min.

Extraction with 2 mL 0.1 M NaOH for 5 min.

and 1580–1590 cm⁻¹ (+0, B+, +BC) reflect the aromatic C=C stretch in simple and polycyclic aromatics, including quinones (Becker et al., 1963) and/or the asymmetric stretch of COO⁻ (Baes and Bloom, 1989). Peaks at 1370 to 1390 cm⁻¹, which are apparent in the spectra of +0, +B and +BC (and as a shoulder in the +C treatment) may be assigned to C-H bending of aliphatics, in-plane O-H bending or symmetric stretching of -COO⁻ (Baes and Bloom, 1989; Cothup et al., 1990). Bands at 1614 and 1508 cm⁻¹ (aromatic C=C stretch), which are apparent in the +C treatment and also in pure catechol (Naidja et al., 1998), are masked by peak broadening for the other treatments. The C-OH stretch of phenolic groups (1270 cm⁻¹) is also most evident in the +C case which contained more unreacted catechol. In contrast, this peak is reduced to a shoulder in +0 and +BC spectra and eliminated in the +B treatment.

The observation that the +C spectrum is similar to

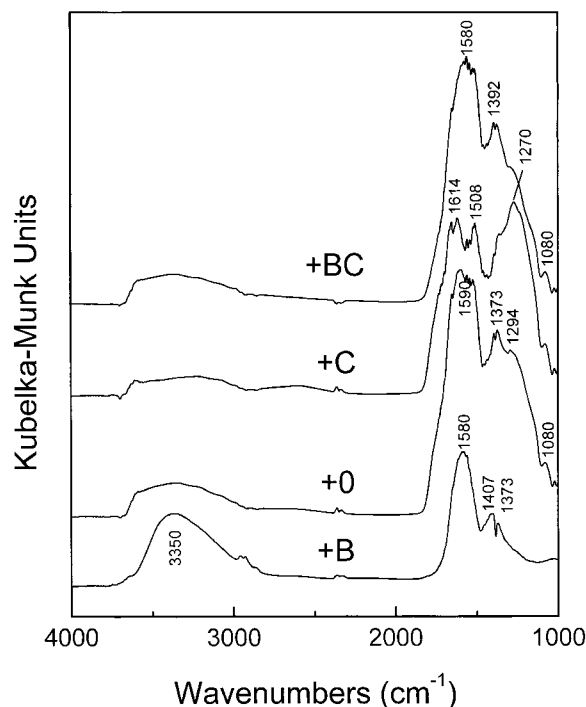


Fig. 4. Diffuse reflectance infrared Fourier transform (DRIFT) difference spectra of solid-phase reaction products. Spectra are the results of subtracting the birnessite spectrum from those of the solid-phase materials.

that of catechol (and different from the remaining treatments) is consistent with diminished catechol transformation measured for the +C case (Fig. 2a). Evidently, although the solid-phase carbon concentration increased when a second dose of catechol was added alone (+C in Fig. 2b), this increase was due, in part, to sorptive retention of unreacted catechol on the pre-existing clay-organic complex. In contrast, addition of a second dose of catechol and birnessite together (+BC) resulted in a very large increase in solid phase carbon. In this case, however, the product spectrum indicates extensive transformation of catechol to give a product that is indistinguishable (on the basis of DRIFT data) from the +0 case. When a second dose of birnessite was added (+B) the peak corresponding to aromatic C=C and/or COO⁻ stretch predominates and the phenolic C-OH stretching vibration is completely eliminated. Hence, the degree of catechol structural transformation as a function of treatment (+B > +0 ≈ +BC > +C) is consistent with the higher CO₂ evolution measured for the +B case (Fig. 2c) and the lower catechol transformation measured for the +C case (Fig. 2a). The band intensity of the C-OH stretch of phenolic groups (1290 cm⁻¹) apparently follows the sequence of unreacted catechol in the various systems.

DISCUSSION

If catechol were oxidized to 1,2-benzoquinone and did not undergo further oxidation, the stoichiometry of the reaction would be given by Eq. [1] and a maximum of 2.3 mmol L⁻¹ of Mn²⁺ would be expected in solution if the reaction goes to completion. Under these conditions, 22% of the initial birnessite mass would be dissolved. However, we observed Mn²⁺ release to be three times greater, consistent with further oxidation of quinone.

Use of ¹⁴C-labeled catechol in kinetic studies of its reaction with birnessite facilitated accounting for its rapid disappearance, the origin and quantity of CO₂ evolved and the mass of partially oxidized reaction products. After 24 h in the baseline treatment (+0, no additions at 5 h), 58 to 61% of the catechol-derived C was in strongly bound, insoluble, solid-phase residues whose structure contained aromatic moieties but less phenolic-OH functionalities than unreacted catechol. The remaining C was in soluble reaction products (16–17%) or released as CO₂ (10–11%).

Although 30 to 40% of the added birnessite was not solubilized by reaction with catechol, the reactivity of the Mn(IV) solids remaining after 5-h reaction time was reduced such that when fresh catechol was added at 5 h (+C) most of this catechol remained unreacted in solution for the duration of the experiment. A small amount of catechol was sorbed to the residual organo-mineral complex, but DRIFT spectra indicated that the sorbed material was structurally similar to catechol and no increases in Mn dissolution or CO₂ evolution were observed. Therefore, the decrease in CO₂ evolution was not simply a result of diminished catechol concentration. Conversely, the oxidation reaction was limited by the availability of reactive birnessite surface. The residual

birnessite may have contained a reduced surface layer (McBride, 1989a) or reactive sites may have been buried by catechol oxidation products. When new birnessite was added at 5 h (+B), a significant increase in CO₂ evolution was observed, along with a smaller increase in Mn dissolution and a reduction in soluble C. Since catechol was undetectable at 5 h, this increase in CO₂ is evidently a result of mineralization of adsorbed catechol and/or residual oxidation products. It is likely that birnessite oxidizes catechol more rapidly than it oxidizes quinone and other initial reaction products and this may affect the extent of CO₂ release under various conditions. For example, Stone and Morgan (1984b) found that 1,4-benzoquinone dissolved Mn oxide, but at a rate that was much slower than hydroquinone. Indeed, the increased CO₂ evolution for the +B case (Fig. 2c) is a result of further oxidation of these initial reaction products.

The presence of residual products (i.e., organo-mineral complexes) can also serve to sequester materials generated by subsequent reactions. When catechol and birnessite were added together at 5-h reaction time (+BC), there was a large increase in Mn dissolution (Fig. 3) but no significant increase in CO₂ evolved relative to the baseline case (Fig. 2c). Despite the presence of fresh substrate and reactive surface, all of the added catechol was rapidly converted into the solid-phase residue (Fig. 2b). Evidently, the residual material remaining from the first 5 h prevented complete oxidation of added catechol by reacting with its initial oxidation products.

On the basis of the results of prior studies (Shindo and Huang, 1982, 1984; Stone, 1987; McBride et al., 1988; McBride, 1989a,b; Wang and Huang, 1994; Naidja et al., 1998) and those reported here, we postulate the following pathway to CO₂ evolution from the oxidation of catechol by Mn(IV) oxides. Electron transfer reactions occur at the mineral surface after formation of a coordinative complex between surface Mn(IV) and phenolic-OH groups (Shindo and Huang, 1982, 1984; Stone and Morgan, 1984a, 1987). The C1 or C2 (hydroxylated) carbon atoms of catechol are the sites of oxidation, ring cleavage and CO₂ release. Accordingly, a minimum of six moles of electrons must be transferred for every mole of CO₂ released, resulting in dissolution of three moles of Mn(II).

As an index of the efficiency of catechol transformation to CO₂ under the different treatments, we calculated the ratio of moles of CO₂ released to moles of Mn dissolved (CO₂/Mn) over time. Assuming (i) a net transfer of 6e⁻ per CO₂ released, (ii) all dissolved Mn is Mn(II), and (iii) once reduced, Mn(II) is not reoxidized or adsorbed, then a molar ratio of 0.33 indicates 100% efficiency [i.e., all Mn(II) production contributes to CO₂ evolution]. Although these assumptions may not all be met, the calculation still provides a useful relative accounting of electron transfer attributable to the competing oxidation pathways under different conditions. After 24 h, the CO₂/Mn ratio for the +B treatment was 0.27 ± 0.02; this suggests that about 80% of the measured Mn dissolution contributed to liberation of CO₂.

Efficiency of catechol mineralization decreased in the other treatment conditions as follows: +B (80%) > +0 (72%) > +C (54%) > +BC (3%). The increase in mineralization efficiency for the +B relative to +0 case suggests that mineralization to CO₂ is limited by reactive birnessite surface area. Furthermore, when a second dose of catechol (+C) or both catechol and birnessite (+BC) is added to a suspension containing residual organo-mineral complexes, these complexes are highly effective at sequestering the new reaction products (partially oxidized organics) before mineralization to CO₂ occurs. With regard to natural soils, the latter point suggests that humic substances (as sequestering agents) would likely reduce the relative proportion of catechol mineralized to CO₂.

REFERENCES

- Baes, A.U., and P.R. Bloom. 1989. Diffuse reflectance and transmission Fourier Transform infrared (DRIFT) spectroscopy of humic and fulvic acids. *Soil Sci. Soc. Am. J.* 53:695–700.
- Becker, E.D., H. Ziffer, and E. Charney. 1963. Molecular vibrations of quinones. I. Fermi resonance involving the carbonyl stretch in *p*-benzoquinones and its isotopic derivatives. *Spectrochim. Acta* 19:1871–1876.
- Bollag, J.-M., C. Myers, S. Pal, and P.M. Huang. 1995. The role of abiotic and biotic catalysts in the transformation of phenolic compounds. p. 299–310. *In* P.M. Huang et al. (ed.) Environmental impact of soil component interactions. Volume 1: Natural and anthropogenic organics. CRC/Lewis Publishers, Boca Raton, FL.
- Bollag, J.-M., K.L. Shuttleworth, and D.H. Anderson. 1988. Laccase-mediated detoxification of phenolic compounds. *Appl. Environ. Microbiol.* 54:3086–3091.
- Chao, T.T. 1972. Selective dissolution of manganese oxides from soils and sediments with acidified hydroxylamine hydrochloride. *Soil Sci. Soc. Am. Proc.* 36:764–768.
- Cheney, M.A., J.Y. Shin, D.E. Crowley, S. Alvey, N. Malengreau, and G. Sposito. 1998. Atrazine dealkylation on a manganese oxide surface. *Colloids Surf.* 137:267–273.
- Cheney, M.A., G. Sposito, A.E. McGrath, and R.S. Criddle. 1996. Abiotic degradation of 2,4-D on synthetic birnessite: A calorimetric method. *Colloids Surfaces* 107:131–140.
- Cothup, N.B., L.H. Daly, and S.E. Wiberley. 1990. Introduction to infrared and Raman spectroscopy. 3rd ed. Academic Press, Boston, MA.
- Dagley, S. 1971. Catabolism of aromatic compounds by microorganisms. *Adv. Microbiol. Physiol.* 6:1–46.
- Huang, P.M. 1991. Kinetics of redox reactions on manganese oxides and its impact on environmental quality. p. 191–230. *In* D.L. Sparks and D.L. Suarez (ed.) Rates of soil chemical processes. SSSA Spec. Publ. 27. SSSA, Madison, WI.
- Lee, J.S.K., and P.M. Huang. 1995. Photochemical effect on the abiotic transformations of polyphenolics as catalyzed by Mn(IV) Oxide. p. 177–189. *In* P.M. Huang et al. (ed.) Environmental impact of soil component interactions. Volume 1: Natural and anthropogenic organics. CRC/Lewis Publishers, Boca Raton, FL.
- Majcher, E.H. 1998. Evolution of ¹⁴C-labeled carbon dioxide from the oxidation of uniformly ¹⁴C-labeled catechol by birnessite. M.S. Thesis, The Pennsylvania State University, University Park, PA.
- Martin, J.P., K. Haider, and L.F. Linhares. 1979. Decomposition and stabilization of ring-¹⁴C-labeled catechol in soil. *Soil Sci. Soc. Am. J.* 43:100–104.
- McBride, M.B. 1987. Adsorption, oxidation of phenolic compounds by Fe and Mn oxides. *Soil Sci. Soc. Am. J.* 5:1466–1472.
- McBride, M.B. 1989a. Oxidation of 1,2- and 1,4-dihydroxybenzene by birnessite in acidic aqueous suspension. *Clays Clay Miner.* 37:479–486.
- McBride, M.B. 1989b. Oxidation of dihydroxybenzenes in aerated suspensions of birnessite. *Clays Clay Miner.* 37:341–347.
- McBride, M.B., F.J. Sikora, and L.G. Wesselink. 1988. Complexation and catalyzed oxidative polymerization of catechol by aluminum in acidic solution. *Soil Sci. Soc. Am. J.* 52:985–993.
- McKenzie, R.M. 1989. Manganese oxides and hydroxides. p. 439–465. *In* J.B. Dixon and S.B. Weed (ed.) Minerals in soil environments. 2nd Ed. SSSA, Madison, WI.
- McKenzie, R.M. 1971. The synthesis of birnessite, cryptomelane, and some other oxides and hydroxides of manganese. *Miner. Mag.* 38:493–502.
- Naidja, A., P.M. Huang, and J.-M. Bollag. 1998. Comparison of reaction products from the transformation of catechol catalyzed by birnessite or tyrosinase. *Soil Sci. Soc. Am. J.* 62:188–195.
- Reineke, W., and H.-J. Knackmuss. 1988. Microbial degradation of haloaromatics. *Annu. Rev. Microbiol.* 42:263–287.
- Shindo, H., and P.M. Huang. 1982. Role of Mn(IV) oxides in abiotic formation of humic substances in the environment. *Nature (London)* 298:363–365.
- Shindo, H., and P.M. Huang. 1984. Catalytic effects of Mn(IV), Fe(III), Al and Si oxides on the formation of phenolic polymers. *Soil Sci. Soc. Am. J.* 48:927–934.
- Silverstein, R.M., G.C. Bassler, and T.C. Morrill. 1991. Spectrometric identification of organic compounds. 5th ed. John Wiley & Sons, New York.
- Stone, A.T. 1987. Reductive Dissolution of Mn(III,IV) oxides by substituted phenols. *Environ. Sci. Technol.* 23:2005–2014.
- Stone, A.T., and J.J. Morgan. 1984a. Reduction of Mn(III), Mn(IV) oxides by organics. A survey of the reactivity of organics. *Environ. Sci. Technol.* 21:979–988.
- Stone, A.T., and J.J. Morgan. 1984b. Reduction and dissolution of Mn(III), Mn(IV) oxides by organics. Reaction with hydroquinone. *Environ. Sci. Technol.* 18:450–456.
- Stone, A.T., and J.J. Morgan. 1987. Reductive dissolution of metal oxides. *In* W. Stumm (ed.) Aqueous surface chemistry. Chemical processes at the particle-water interface. p. 221–253. John Wiley & Sons, New York.
- Wang, M.C. 1995. Influence of Pyrogallol on the Catalytic Action of Iron and Manganese Oxides in Amino Acid Transformation. p. 169–175. *In* P.M. Huang et al. (ed.) Environmental impact of soil component interactions. Volume 1: Natural and anthropogenic organics. CRC/Lewis Publishers, Boca Raton, FL.
- Wang, M.C., and P.M. Huang. 1994. Structural Role of polyphenols in influencing the ring cleavage and related chemical reactions as catalyzed by nontronite. p. 173–180. *In* N. Senesi and T.M. Miano (ed.) Humic substances in the global environment and implications on human health. Elsevier, New York.